J|A|C|S
ARTICLES
Published on Web 07/10/2002

Intramolecular Quenching of Tryptophan Fluorescence by the Peptide Bond in Cyclic Hexapeptides

Paul D. Adams,[‡] Yu Chen,[†] Kan Ma,[‡] Michael G. Zagorski,[‡] Frank D. Sönnichsen,[§] Mark L. McLaughlin,[⊥] and Mary D. Barkley*,[‡]

Contribution from the Departments of Chemistry and Physiology and Biophysics, Case Western Reserve University, Cleveland, Ohio 44106, and Department of Chemistry, Louisiana State University, Baton Rouge, Louisiana 70803

Received August 6, 2001

Abstract: Intramolecular quenching of tryptophan fluorescence by protein functional groups was studied in a series of rigid cyclic hexapeptides containing a single tryptophan. The solution structure of the canonical peptide c[D-PpYTFWF] (pY, phosphotyrosine) was determined in aqueous solution by 1D- and 2D-^{1}H NMR techniques. The peptide backbone has a single predominant conformation. The tryptophan side chain has three χ_1 rotamers: a major $\chi_1 = -60°$ rotamer with a population of 0.67, and two minor rotamers of equal population. The peptides have three fluorescence lifetimes of about 3.8, 1.8, and 0.3 ns with relative amplitudes that agree with the χ_1 rotamer populations determined by NMR. The major 3.8-ns lifetime component is assigned to the $\chi_1 = -60°$ rotamer. The multiple fluorescence lifetimes are attributed to differences among rotamers in the rate of excited-state electron transfer to peptide bonds. Electron-transfer rates were calculated for the six preferred side chain rotamers using Marcus theory. A simple model with reasonable assumptions gives excellent agreement between observed and calculated lifetimes for the 3.8- and 1.8-ns lifetimes and assigns the 1.8-ns lifetime component to the $\chi_1 = 180°$ rotamer. Substitution of phenylalanine by lysine on either side of tryptophan has no effect on fluorescence quantum yield or lifetime, indicating that intramolecular excited-state proton transfer catalyzed by the ϵ-ammonium does not occur in these peptides.

Tryptophan fluorescence has been used extensively to study peptide and protein conformation changes, due to the sensitivity of both emission wavelength and intensity to the local environment of the indole chromophore. The wavelength of maximum emission ranges from about 310−350 nm, depending on the electrostatic environment.[1] The fluorescence quantum yield ranges from near zero to 0.35 with lifetimes up to 10 ns.[2,3] The large variations in intensity and fluorescence lifetime τ are due to nonradiative pathways that compete with emission for deactivation of the excited state.

$$\tau^{-1} = k_r + k_{nr} \quad (1)$$

where k_r and k_{nr} are the radiative and nonradiative rates. In addition to the intersystem crossing rate k_{isc}, the nonradiative rate of indole contains contributions from three environmentally sensitive processes, solvent quenching k_{si}, excited-state proton transfer k_{pt}, and excited-state electron transfer k_{et}, which depend on the proximity of water, proton donors, and electron acceptors.[4−7]

$$k_{nr} = k_{isc} + k_{si} + k_{pt} + k_{et} \quad (2)$$

Six protein functional groups representing eight amino acid side chains plus the peptide bond quench 3-methylindole fluorescence in intramolecular quenching experiments.[8] Most peptides and proteins containing a single tryptophan have multiexponential fluorescence decays. Although excited-state processes are still invoked to account for the complexity,[9−12] the multiple fluorescence lifetimes are generally attributed to ground-state heterogeneity.[13] The rotamer model proposes that the multiple lifetimes represent multiple ground-state rotamers of the tryp-

* Address correspondence to this author at Department of Chemistry, Case Western Reserve University, 10900 Euclid Avenue, Cleveland, OH 44106-7078. Fax: 216-368-0604. E-mail: mdb4@po.cwru.edu.
[‡] Department of Chemistry, Case Western Reserve University.
[†] Current address: BD Pharmingen, 10975 Torreyana Road, San Diego, CA 92121.
[§] Department of Physiology and Biophysics, Case Western Reserve University.
[⊥] Louisiana State University.

(1) Callis, P. R.; Burgess, B. K. *J. Phys. Chem. B* **1997**, *101*, 9429−9432.
(2) Beechem, J. M.; Brand, L. *Annu. Rev. Biochem.* **1985**, *54*, 43−71.
(3) Eftink, M. R. *Methods Biochem. Anal.* **1991**, *35*, 127−205.
(4) Saito, I.; Sugiyama, H.; Yamamoto, A.; Muramatsu, S.; Matsuura, T. *J. Am. Chem. Soc.* **1984**, *106*, 4286−4287.
(5) McMahon, L. P.; Colucci, W. J.; McLaughlin, M. L.; Barkley, M. D. *J. Am. Chem. Soc.* **1992**, *114*, 8442−8448.
(6) Yu, H.-T.; Colucci, W. J.; McLaughlin, M. L.; Barkley, M. D. *J. Am. Chem. Soc.* **1992**, *114*, 8449−8454.
(7) Chen, Y.; Liu, B.; Yu, H.-T.; Barkley, M. D. *J. Am. Chem. Soc.* **1996**, *118*, 9271−9278.
(8) Chen, Y.; Barkley, M. D. *Biochemistry* **1998**, *37*, 9976−9982.
(9) Ladokhin, A. S. *J. Fluoresc.* **1999**, *9*, 1−9.
(10) Hudson, B. S.; Huston, J. M.; Soto-Campos, G. *J. Phys. Chem. A* **1999**, *103*, 2227−2234.
(11) Moncrieffe, M. C.; Juranic, N.; Kemple, M. D.; Potter, J. D.; Macura, S.; Prendergast, F. G. *J. Mol. Biol.* **2000**, *297*, 147−163.
(12) Nanda, V.; Brand, L. *Proteins* **2000**, *40*, 112−125.
(13) Sillen, A.; Díaz, J. F.; Engelborghs, Y. *Protein Sci.* **2000**, *9*, 158−169.

10.1021/ja0167710 CCC: $22.00

tophan side chain.[14,15] There are six low-energy canonical conformations dictated by the torsional angles about the $C^{\alpha}-C^{\beta}$ ($\chi_1 = \pm 60°, 180°$) and $C^{\beta}-C^{\gamma}$ ($\chi_2 = \pm 90°$) bonds. If proximity of the indole ring to water or quenching functional groups differs among rotamers, those rotamers will have different fluorescence lifetimes. If interconversion among rotamers is slower than the fluorescence time scale, the fluorescence decay will be multiexponential with relative amplitudes proportional to the rotamer populations. For small peptides in solution or bound to membrane vesicles, several groups have proposed that the two or three fluorescence decay components represent χ_1 rotamers.[16−19] The three decay amplitudes of [Trp^2]oxytocin were correlated with χ_1 rotamer populations determined by ^{1}H NMR.[20] In addition to rotamers of the tryptophan side chain, microconformational states of peptides and proteins with different local environments of the indole ring constitute a source of ground-state heterogeneity. Finally, relaxation of the protein matrix surrounding the indole ring during the lifetime of the excited state would also produce a complex decay.

This contribution tests the rotamer model in a cyclic hexapeptide containing a single tryptophan and five other amino acids whose side chains do not quench 3-methylindole fluorescence. The cyclic peptide is closely related to a somatostatin analogue previously shown to have a rigid backbone in organic solvent.[21] The solution structure of the cyclic peptide in aqueous solution is determined by 1D- and 2D-^{1}H NMR. The tryptophan fluorescence is characterized by steady-state and time-resolved techniques, and the dependence on solvent isotope and temperature is determined. Fluorescence decay amplitudes are correlated with the NMR-determined χ_1 rotamer populations of the tryptophan side chain. Excited-state electron-transfer rates for intramolecular quenching of the six χ_1, χ_2 rotamers by the peptide bonds are calculated from Marcus theory using distances estimated by molecular modeling and parameters estimated from the electron-transfer rate of *N*-acetyltryptophanamide (NATA). The fluorescence lifetimes of the six rotamers are calculated using these electron-transfer rates together with experimental values for the intersystem-crossing and water-quenching rates previously determined for NATA.[7] The observed fluorescence decay is interpreted in terms of the χ_1 rotamer populations and the calculated χ_1, χ_2 rotamer lifetimes.

Experimental Section

Materials. Oxime resin was either purchased from Novabiochem or synthesized.[22] *N*-α-*t*-Boc-D-proline, -L-phenylalanine, -L-tryptophan, -L-threonine, and -L-leucine, *N*-α-*t*-Boc-*N*-ϵ-benzyloxycarbonyl-L-lysine, 2-(1*H*-benzotriazole-1-yl)-1,1,3,3-tetramethyluronium hexafluorophosphate (HBTU), and *N*-hydroxybenzotriazole·H_2O (HOBT) were purchased from Novabiochem. *N*-α-*t*-Boc-L-phosphotyrosine·diisopropylethylamine was purchased from Advanced Chemtech. *O*-(7-azabenzotriazol-1-yl)-1,1,3,3-tetramethyluronium hexafluorophosphate (HATU) was purchased from Perceptive Biosystems. All other reagents and solvents were highest grade available.

Synthesis. Peptides were synthesized manually using oxime resin at 25 °C.[23] The oxime resin offers two advantages for the synthesis of small cyclic peptides containing tryptophan: simultaneous cyclization and cleavage from the resin under mild conditions and efficient isolation from multimeric side products.[22,23] The disadvantage of using Boc resins is that the repetitive trifluoroacetic acid (TFA) deprotection may result in modification of peptide side chains. The extent of cyclization using the oxime resin is highly sequence-dependent.[24] Therefore, the amino acid that was coupled to the resin was permuted in the sequence c[D-PpYTFWF] except for D-Pro^1 and pTyr^2 (phosphotyrosine, pY). The synthesis starting with Thr^3 gave the best overall yield of purified peptide. Thr (3 mmol) was coupled to 1 g of resin (substitution level 0.3−0.5 mmol/g) using 0.35 mM diisopropylcarbodiimide in 6 mL of CH_2Cl_2 for 24 h. The solvent was removed, and unreacted sites on the oxime resin were capped by addition of 6 mL of dry dimethylformamide (DMF) containing 0.2 M acetic or trimethylacetic anhydride and 0.3 M diisopropylethylamine (DIEA). The coupled amino acid was deprotected with 25% TFA in 4−6 mL of CH_2Cl_2 for 15−20 min. Amino acid coupling reactions were carried out by shaking at room temperature for 45 min in 6 mL of dry DMF containing 0.25 M HBTU, 0.1 M HOBT, and 0.5 M DIEA, except for D-Pro where HATU replaced HBTU. The extent of coupling was monitored by a ninhydrin color test on a small aliquot of resin after each step.[25] After the last deprotection, the peptide was cyclized and cleaved from the resin by reaction for 48 h with 0.5 M acetic acid and 1.5 M triethylamine in 6−8 mL of dry DMF.[26] For c[D-PpYTFWF] and c[D-PpYTFLF], the organic phase was removed by filtration and added dropwise to cold diethyl ether, and the white precipitate was removed by centrifugation. Alternatively, the DMF was removed by vacuum distillation, which gave a viscous orange residue. For c[D-PFTK(z)WF] and c[D-PFTFWK(z)], the organic layer was added dropwise to cold water, and the white precipitate was removed by centrifugation. The resulting pellet or residue was dissolved in a small volume of 1:1 CH_3CN/H_2O and purified by RP-HPLC on a Vydac C-18 semi-prep column using a gradient of CH_3CN/0.1% TFA: 20−55% for 60 min for c[D-PpYTFWF] and 40−100% for 40 min for the other peptides.

Deprotection of the ϵ-amino group of lysine was done by catalytic hydrogenation. The peptide was dissolved in a minimal volume (5−10 mL) of glacial acetic acid and placed in a hydrogenation flask. A catalytic amount of 10% Pd on carbon was added, and the suspension was purged with argon three times and then charged to 50 psi with hydrogen and shaken overnight. After the hydrogenation was complete, the Pd catalyst was filtered off, and the flask was washed five times with small aliquots of ethyl acetate. The ethyl acetate/acetic acid solvent was removed under vacuum to yield the crude, yellow deprotected peptide. The peptides were purified by HPLC using a gradient of 20−55% CH_3CN/0.1% TFA for 60 min.

Peptide molecular weights were verified by MALDI-MS. Yields of purified peptide were 8−17% relative to the substitution level of the oxime resin. The low yields are probably due to TFA-mediated side chain reactions or cleavage of the linear sequence during the cyclization step.

^{1}H Nuclear Magnetic Resonance. All NMR experiments were performed using a Varian Inova 600 MHz spectrometer. For experiments in H_2O, 2 mg of peptide was dissolved in 600 μL of 10 mM phosphate buffer, 1 mM NaN_3, 10% D_2O and pH was adjusted to 3−5 with dilute HCl. Chemical shifts were referenced to 3-(trimethylsilyl)-propanate-2,2,3,3-d_4 (TSP). For experiments in 100% D_2O, 1 mg of

(14) Donzel, B.; Gauduchon, P.; Wahl, P. *J. Am. Chem. Soc.* **1974**, *96*, 801−808.
(15) Szabo, A. G.; Rayner, D. M. *J. Am. Chem. Soc.* **1980**, *102*, 554−563.
(16) Willis, K. J.; Szabo, A. G. *Biochemistry* **1992**, *31*, 8924−8931.
(17) Willis, K. J.; Neugebauer, W.; Sikorska, M.; Szabo, A. G. *Biophys. J.* **1994**, *66*, 1623−1630.
(18) Dahms, T. E. S.; Willis, K. J.; Szabo, A. G. *J. Am. Chem. Soc.* **1995**, *117*, 2321−2326.
(19) Clayton, A. H.; Sawyer, W. H. *Biophys. J.* **1999**, *76*, 3235−3242.
(20) Ross, J. B. A.; Wyssbrod, H. R.; Porter, R. A.; Schwartz, G. P.; Michaels, C. A.; Laws, W. R. *Biochemistry* **1992**, *31*, 1585−1594.
(21) Kessler, H.; Bats, J. W.; Griesinger, C.; Koll, S.; Will, M.; Wagner, K. *J. Am. Chem. Soc.* **1988**, *110*, 1033−1049.
(22) DeGrado, W. F.; Kaiser, E. T. *J. Org. Chem.* **1980**, *45*, 1295−1300.
(23) Osapay, G.; Bouvier, M.; Taylor, J. W. *Technol. Protein Chem. 2* **1991**, 221−231.
(24) Nishino, N.; Xu, M.; Mihara, H.; Fujimoto, T. *Tetrahedron Lett.* **1992**, *33*, 1479−1482.
(25) Kaiser, E. T.; Colescott, R. L.; Bossinger, C. D.; Cook, P. I. *Anal. Biochem.* **1970**, *34*, 595−598.
(26) Gisin, B. F.; Merrifield, R. B. *J. Am. Chem. Soc.* **1972**, *94*, 3102−3106.

peptide was dissolved in 270 μL of D_2O (Cambridge Isotope) in a Shigemi NMR tube. Chemical shifts δ of amide protons were measured in 5° increments from 5 to 55 °C. Temperature coefficients $-d\delta/dT$ were determined from the slope of a plot of chemical shift vs temperature by least-squares.

Spin-type assignments for c[D-PpYTFWF] were made from TOCSY spectra[27,28] that used a mixing time of 70 ms, spectral width of 7000.4 Hz, and 2048 data points in 256 t_1 increments of 24 transients. Water suppression was performed by low-power irradiation with a presaturation delay pulse of 1 s. NOESY spectra[29] used mixing times up to 300 ms and WATERGATE water suppression sequence.[30] NOESY spectra were acquired with 1024 data points in 256 t_1 increments of 32 transients. Interproton distances from NOESY experiments were calculated using the isolated two-spin approximation theory.[31] A reference distance of 2.82 Å from the indole NH to H7 of the indole ring was taken from the crystal structure.[32] PE-COSY spectra[33] were acquired with a spectral width of 6600 Hz and 4096 data points in 440 t_1 increments of 80 transients.

NMR data were processed using the Felix program (Molecular Simulations, Inc.) on an INDY-IP22 work station (Silicon Graphics, Inc.). Convolution difference water deconvolution was used to remove the residual water signal in the spectra. Data were routinely zero-filled to 2K data points in both dimensions, with the exception of the PE-COSY, which was filled to 8K in D1 dimension and 2K in D2 dimension. In all spectra, a Gaussian and a 90°-shifted sinebell squared apodization function were used in the D1 and D2 dimension, respectively. The data were then phase corrected and baseline corrected.

Structure calculations were performed using the NMR-Refine module of InsightII (Molecular Simulations, Inc.). A set of 30 structures was generated in DGII from 59 NOE-derived distance restraints comprising 23 intraresidue, 23 sequential, and 13 nonadjacent restraints, two hydrogen bond restraints, 13 ^3J dihedral angle restraints, and six chiral restraints.[34] The NOE restraints were grouped as strong, medium, and weak, which corresponded to 1.8−2.7, 1.8−3.3, and 1.8−5.0 Å distance ranges. The two hydrogen bond restraints were incorporated on the basis of the reduced temperature coefficients for the amide protons of Thr^3 and Phe^6. They were defined as O···N distance ranges of 2.6−3.2 Å between residues 3 and 6.[35] These restraints did not bias the structure calculations as judged by repeating the calculations without hydrogen bond restraints. The DGII calculation was done using 10,000 steps of simulated annealing and 500 steps of conjugate gradient optimization to an RMS gradient of 0.001. Structures were further minimized in Discover using the CVFF force field and a dielectric constant of 78.0 for water.[36] A 500-step steepest descent minimization without cross and Morse potentials was performed until the maximum derivative was 10.0 kcal/Å, followed by a 1000-step conjugate gradients minimization until the maximum derivative was 1.0 kcal/Å. Finally, a 5000-step VA09A minimization using cross and Morse terms was performed until the maximum derivative was 0.001 kcal/Å. The final ensemble consisted of the 17 lowest-energy structures.

Molecular Modeling. Six canonical rotamers of the tryptophan side chain in NATA and c[D-PpYTFWF] were modeled having $\chi_1 = \pm 60°$, 180° and $\chi_2 = \pm 90°$. The distance from a pseudoatom between C8 and C9 of the indole ring to each carbonyl carbon in the molecule was measured in InsightII. The dihedral angle between the planes of the indole ring and each peptide group was measured in the Decipher module. Twelve starting structures for NATA were constructed in Biopolymer with the ϕ,ψ angles rotated in 30° increments from 0 to 360° to simulate unrestricted backbone rotation. The mean structure of c[D-PpYTFWF] determined above was used as starting structure for the cyclic peptide. Six tryptophan rotamers were generated for each starting structure. The resulting structures were minimized in Discover with χ_1 and χ_2 constrained to canonical values, and the distances and angles between the indole ring and the peptide groups were measured.

Fluorescence Spectroscopy. Steady-state and time-resolved fluorescence measurements were made as before.[5,7,37] All experiments were performed on aqueous solutions with absorbance <0.1 at 280 nm. Absorbance was measured on a Cary 3E UV−vis spectrophotometer. Steady-state fluorescence was measured on a SLM 8000 photon counting spectrofluorimeter in ratio mode. Fluorescence quantum yields Φ were determined at 280- and 295-nm excitation wavelength (4-nm band-pass). Quantum yields were measured relative to tryptophan (Sigma, recrystallized four times from 70% ethanol) in H_2O using a value of 0.14 at 25 °C.[38] The absorbance of Trp^5-containing peptides was corrected for contributions from pTyr and Phe by subtracting the absorbances at 280 and 295 nm of a control peptide c[D-PpYTFLF] at the same concentration. Peptide concentrations were determined by quantitative amino acid analysis. The absorbance of the control peptide was <5% of Trp^5-containing peptides at 280 nm and negligible at 295 nm.

Time-resolved fluorescence was measured by time-correlated single photon counting using a rhodamine 6G dye laser excitation source. Excitation wavelength was 295 nm. Fluorescence decays were collected at 10-nm increments from 320 to 390 nm emission wavelength (8-nm band-pass). Temperature dependence data were collected at 360 nm emission wavelength in 5° increments from 5 to 55 °C. Data were acquired from the fluorescent sample and a solution of coffee creamer in water for the instrumental response to $1.8-2.5 \times 10^4$ counts in the peak. Decay data were stored in 1024 channels of 10 and 24 ps/channel.

Decay curves were deconvolved assuming a discrete sum of exponentials in the Beechem global analysis program[39]

$$I(\lambda,t) = \sum_i \alpha_i(\lambda) \exp(-t/\tau_i) \quad (3)$$

where $\alpha_i(\lambda)$ is the amplitude at wavelength λ and τ_i is the lifetime of component i. Lifetimes but not amplitudes were linked in global analyses. Individual decay curves were also deconvolved by the maximum entropy method (MEM).[40]

$$I(\lambda,t) = \int_0^\infty \alpha(\lambda,\tau) \exp(-t/\tau)\, d\tau \quad (4)$$

where $\alpha(\lambda,\tau)$ is the fluorescence lifetime distribution at wavelength λ. Quality of fit was judged by the value of reduced χ_r^2, the weighted residuals, and the shape of the autocorrelation function of the weighted residuals. Decay curves were simulated with 1.8×10^4 counts in the peak using experimental instrumental response functions of 10 and 24 ps/channel in the Beechem program.The radiative rate k_r is calculated from

$$k_r = \Phi/\bar{\tau} \quad (5)$$

where $\bar{\tau}$ is the average lifetime

$$\bar{\tau} = \sum_i \alpha_i(\lambda)\, \tau_i / \sum_i \alpha_i(\lambda) \quad (6)$$

Results and Discussion

Backbone Conformation of c[D-PpYTFWF]. The ground-state structure of a closely related peptide, c[D-PFTK(z)WF],

(27) Bax, A.; Davis, D. G. *J. Magn. Reson.* **1985**, *65*, 355−360.
(28) Shaka, A. S.; Lee, C. J.; Pines, A. *J. Magn. Reson.* **1988**, *77*, 274−293.
(29) Kumar, A.; Ernst, R. R.; Wuthrich, K. *Biochem. Biophys. Res. Commun.* **1980**, *95*, 1−6.
(30) Piotto, M.; Saudek, V.; Sklenar, V. *J. Biomol. NMR* **1992**, *2*, 661−665.
(31) Wüthrich, K. *NMR of Proteins and Nucleic Acids*; Wiley: New York, 1986.
(32) Bye, E.; Mostad, A.; Romming, C. *Acta Chem. Scand.* **1973**, *27*, 471−484.
(33) Mueller, L. *J. Magn. Reson.* **1987**, *72*, 191−196.
(34) Havel, T. F.; Kuntz, I. D.; Crippen, G. M. *Bull. Math. Biol.* **1983**, *45*, 665−720.
(35) Talafous, J.; Marcinowski, K. J.; Klopman, G.; Zagorski, M. G. *Biochemistry* **1994**, *33*, 7788−7795.
(36) *NMRchitect*; Biosym/MSI: San Diego, 1995.
(37) Liu, B.; Thalji, R. K.; Adams, P. D.; Fronczek, F. R.; McLaughlin, M. L.; Barkley, M. D. *J. Am. Chem. Soc.* **2001**, in revision.
(38) Chen, R. F. *Anal. Lett.* **1967**, *1*, 35−42.
(39) Beechem, J. M. *Chem. Phys. Lipids* **1989**, *50*, 237−251.
(40) Brochon, J.-C. *Methods Enzymol.* **1994**, *240*, 262−311.

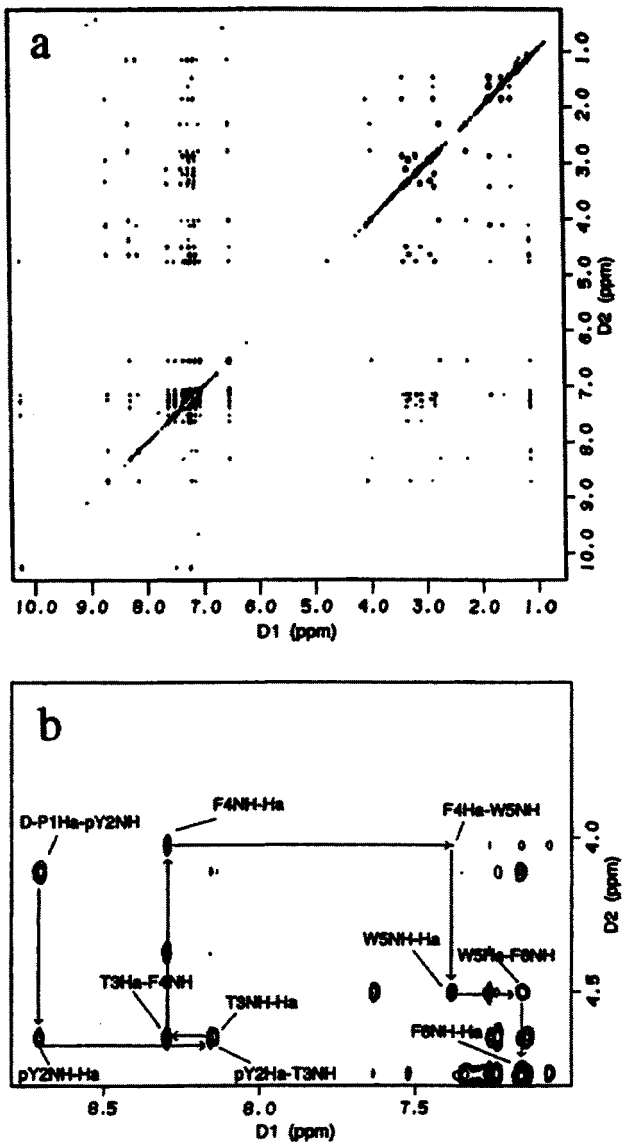

Figure 1. ^{1}H,^{1}H NOESY spectrum of c[D-PpYTFWF] in 10 mM phosphate buffer, pH 3, 25 °C. (a) Entire spectrum. (b) Expansion showing NH−Hα cross-peaks. Sequential connectivities are indicated by lines.

in DMSO was reported by Kessler et al.[21] The salient features of the Kessler peptide are (1) a rigid peptide with a single predominant backbone conformation and a *trans* conformation of the Phe^6-D-Pro^1 peptide bond from the H,C COSY spectrum, (2) a βI turn about Lys^4−Trp^5 and a βII′ turn about D-Pro^1-Phe^2 determined from $^3J_{NH-H\alpha}$ coupling constants and ROE data, and (3) two intramolecular hydrogen bonds between Thr^3-CO···NH-Phe^6 and Phe^6-CO···NH-Thr^3 inferred from temperature dependence of amide proton chemical shifts.

A similar approach was used to determine the structure of c[D-PpYTFWF] in aqueous solution. There is only one set of proton resonances in the 1D-spectra from 5 to 55 °C and in the TOCSY spectrum of c[D-PpYTFWF] in H_2O. The NOESY spectrum at 25 °C was used to make sequential assignments as well as to measure interproton distances (Figure 1a). Sequential assignments from NH−Hα cross-peaks were used to identify the NH, Hα, and Hβ resonances of Phe^4 and Phe^6, because the ring protons for the Phe residues were indistinguishable (Figure 1b). A *trans* peptide bond about Phe^6-D-Pro^1 is evident from the two NOE cross-peaks between the Hα proton of Phe^6 and the Hδ protons of D-Pro^1.[41] The 1D-spectra of c[D-PFTKWF] and c[D-PFTFWK] had NH and Hα chemical shifts very similar to those of c[D-PpYTFWF].

Table 1. NMR Data

	−dδ/dT (ppb/deg)	$^3J_{NH-H\alpha}$ (Hz)	$^3J_{H\alpha-H\beta r}$ (Hz)	$^3J_{H\alpha-H\beta s}$ (Hz)	pI	pII	pIII
c[D-PpYTFWF] in water							
D-Pro^1							
pTyr^2	8.7	8.5	10.2	4.8	0.70	0.19	0.11
Thr^3	3.9	9.6					
Phe^4	5.5	3.3	6.8	7.9	0.38	0.57	0.05
Trp^5	4.6	8.4	9.9	4.4	0.67	0.16	0.17
Phe^6	0.9	7.8					
c[D-PFTK(z)WF] in DMSO[a]							
D-Pro^1							
Phe^2	7.0	8.9	11.5	3.1	0.80	0.05	0.15
Thr^3	3.3	9.7					
Lys(z)^4	4.3	3.4					
Trp^5	3.0	8.9	10.9	4.2	0.75	0.15	0.10
Phe^6	1.0	5.8	4.5	9.0	0.17	0.58	0.25

[a] Data from ref 21.

The β-turns of the Kessler peptide are preserved in c[D-PpYTFWF], with a βI turn about Phe^4-Trp^5 and a βII′ turn about D-Pro^1-pTyr^2. Vicinal $^3J_{NH-H\alpha}$ coupling constants from 1D-spectra of c[D-PpYTFWF] in H_2O are similar to the coupling constants for c[D-PFTK(z)WF] in DMSO (Table 1). The upfield shifted D-Pro^1 Hα resonance at 4 ppm is additional evidence for a β-turn about D-Pro^1-pTyr^2.[42] The small temperature coefficient of the Phe^6-NH chemical shift suggests one intramolecular hydrogen bond at Thr^3-CO···NH-Phe^6 as found in the Kessler peptide (Table 1). The temperature coefficient of Thr^3-NH in the intermediate range is consistent with the other hydrogen bond suggested by Kessler.[21]

Two facts point to a single backbone conformation for c[D-PpYTFWF] in aqueous solution. First, there is no detectable *cis*−*trans* isomerization of the Phe^6-D-Pro^1 peptide bond in the NMR data. Second, four of five $^3J_{NH-H\alpha}$ coupling constants in Table 1 fall outside the 6−8 Hz range attributed to conformational averaging. The overall structure of c[D-PpYTFWF] was generated from distance geometry calculations using restraints derived from NOE and *J* coupling data. There were no NOE distance restraint violations greater than 0.5 Å in the distance geometry calculations. The average structure from the family of 17 structures is shown in Figure 2. The average overall backbone RMSD is 0.43 ± 0.05 Å; the all-atom RMSD is 1.90 ± 0.06 Å.

Side Chain Conformation. The rotamer populations for $\chi_1 = \pm 60°, 180°$ conformations of amino acid side chains in c[D-PpYTFWF] were calculated from $^3J_{H\alpha-H\beta}$ coupling constants using the Pachler equations.[43] Coupling constants for Phe^4 and Trp^5 were determined from the 1D-spectrum; coupling constants for pTyr^2 were determined from the PE-COSY spectrum. Table 1 compares the χ_1 rotamer populations pI−III for c[D-PpYTFWF] in D_2O and c[D-PFTK(z)WF] in DMSO. The populations for amino acids at the same position in the sequence are similar in the two peptides. Trp^5 adopts a major χ_1 side chain conformation with two equally populated minor conformations.

(41) Kessler, H.; Anders, U.; Schudok, M. *J. Am. Chem. Soc.* **1990**, *112*, 5908−5916.
(42) Stroup, A. N.; Rockwell, A. L.; Gierasch, L. M. *Biopolymers* **1992**, *32*, 1713−1725.
(43) Pachler, K. G. R. *Spectrochim. Acta* **1963**, *19*, 2085−2092.

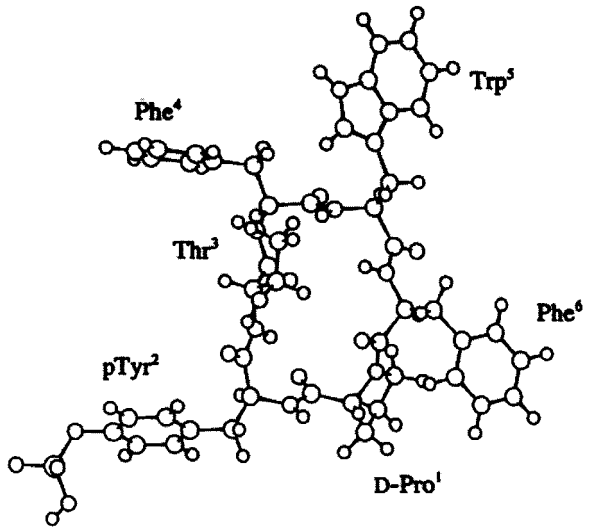

Figure 2. Mean structure of c[D-PpYTFWF] from distance geometry and energy minimization calculations.

The NOESY spectrum showed a single set of cross-peaks between Hα and Hβ protons of Trp[5], consistent with fast averaging of the side chain conformation on the NMR time scale. A semiquantitative analysis of local NOE intensities facilitated stereospecific assignments of the Trp[5] Hβ protons and identification of the major χ_1 rotamer as $-60°$, under the basic assumption that a major χ_1 rotamer dominates the cross-peak intensities.[44] The NOE intensity is about 1.5-fold larger for the Hα−Hβs cross-peak than for the Hα−Hβr cross-peak of Trp[5]. There is also 1.4-fold stronger NOE intensity between Trp[5] amide NH−Hβr than NH−Hβs. These two NOE intensity ratios indicate a predominant conformation with $\chi_1 = -60°$.

The presence of multiple interconverting χ_1 rotamers makes it impossible to determine χ_2 rotamer populations for each χ_1 rotamer. NOE intensities alone can be interpreted at best semiquantitatively. Nevertheless, NOE intensities between the two Trp Hβ protons and the indole ring H2 and H4, which depend solely on χ_2 conformation, occur with comparable intensities in all data, suggesting little χ_2 preference for Trp[5] in this peptide. The presence of both H2 and H4 cross-peaks with Hα, which indicate primarily χ_1, $\chi_2 = 60°$, $-90°$; 180°, 90° and χ_1, $\chi_2 = -60°$, 90°; 180°, $-90°$, respectively, excludes correlation between χ_1 and χ_2. The data suggest the presence of up to six Trp[5] side chain rotamers in c[D-PpYTFWF].

Fluorescence Spectroscopy. The fluorescence emission maxima λ_{max} and quantum yields Φ of c[D-PpYTFWF], c[D-PFTKWF], and c[D-PFTFWK] in H_2O and D_2O are given in Table 2. The broad, featureless emission spectra of the peptides are essentially identical to the spectrum of NATA in aqueous solution. The quantum yields of the peptides and NATA are the same within error. The values are slightly higher in D_2O than H_2O with the same 1.2-fold solvent isotope effect.[5] The only functional groups in the peptides and NATA that quench 3-methylindole fluorescence in intermolecular quenching experiments are the amide groups.[7,8] Intramolecular quenching by the peptide bonds in NATA is due to excited-state electron transfer.[7]

Fluorescence decays were measured for c[D-PpYTFWF], c[D-PFTKWF], and c[D-PFTFWK] in H_2O and D_2O at 25 °C. Time-resolved emission spectral data collected on two time scales were deconvolved in global analyses with the lifetimes linked. The decay curves for the peptides gave good fits to three exponential functions with χ_r^2 values of 1.4−1.6 and lifetimes of about 3.8, 1.8, and 0.3 ns in H_2O (Table 3). Triple exponential fits were an improvement over double exponential fits, which had χ_r^2 values of 1.9 and nonrandom weighted residuals and autocorrelation functions. MEM analysis, in which the decay model is not predetermined, supports a triple exponential decay. The relative amplitudes α_i appear independent of emission wavelength: about 0.7 for the 3.8-ns component, 0.16 for the 1.8-ns component, and 0.14 for the 0.3-ns component. These amplitudes correlate very well with the χ_1 rotamer populations determined from $^3J_{H\alpha-H\beta}$ coupling constants (Table 1), which associates the 3.8-ns lifetime component with the $\chi_1 = -60°$ rotamer.

Radiative and nonradiative rates were calculated from quantum yield and lifetime data using eqs 1, 5, and 6. Intramolecular static quenching in dipeptides reduces the apparent value of k_r for tryptophan below the value for NATA.[45] The radiative rates k_r for the cyclic peptides and NATA are about the same and independent of solvent isotope within error (Table 2). Thus, Trp[5] does not undergo ground-state interactions in the cyclic peptides that create a nonfluorescent population of tryptophan residues. The nonradiative rates k_{nr} are slightly higher in H_2O than D_2O due to water quenching, which is an isotopically sensitive temperature-dependent quenching process.[5] The finding of the same quantum yields, lifetimes, and deuterium isotope

Table 2. Fluorescence Data[a]

solvent	λ_{max} (nm)	Φ_{280}[b]	Φ_{295}[b]	$\bar{\tau}$[c] (ns)	k_r[d] (10^7 s^{-1})	k_{nr} (10^7 s^{-1})
			c[D-PpYTFWF]			
H_2O	348	0.17 ± 0.02	0.17 ± 0.02	2.9 ± 0.1	5.7 ± 0.7	28 ± 2
D_2O	350	0.20 ± 0.02	0.21 ± 0.03	3.21 ± 0.06	6.5 ± 0.9	25 ± 1
			c[D-PFTKWF]			
H_2O	350	0.16 ± 0.02	0.17 ± 0.02	3.06 ± 0.09	5.5 ± 0.7	27 ± 1
D_2O	350	0.20 ± 0.01	0.21 ± 0.02	3.30 ± 0.06	6.4 ± 0.6	23.9 ± 0.8
			c[D-PFTFWK]			
H_2O	349	0.17 ± 0.01	0.18 ± 0.01	2.9 ± 0.2	6.1 ± 0.5	28 ± 2
D_2O	351	0.19 ± 0.01	0.22 ± 0.01	3.2 ± 0.1	6.9 ± 0.4	24 ± 1
			NATA[e]			
H_2O	350	0.15 ± 0.02		2.6 ± 0.4	6 ± 1	33 ± 6
D_2O	350	0.18 ± 0.03		3.3 ± 0.5	5 ± 1	25 ± 5

[a] 25 °C. [b] Mean values with standard deviations from 5 to 20 experiments. [c] Values for cyclic peptides calculated from lifetime data in Table 3. [d] Values for cyclic peptides calculated using quantum yields measured at 295 nm excitation wavelength. [e] Data from ref 66.

Table 3. Fluorescence Lifetime Data[a]

solvent	α_1	τ_1 (ns)	α_2	τ_2 (ns)	τ_3 (ns)	χ_r^2
			c[D-PpYTFWF]			
H_2O	0.68 ± 0.03	3.82	0.17 ± 0.02	1.83	0.32	1.5
D_2O	0.66 ± 0.05	4.25	0.16 ± 0.02	2.02	0.45	1.5
			c[D-PFTKWF]			
H_2O	0.70 ± 0.02	3.91	0.16 ± 0.02	1.84	0.28	1.6
D_2O	0.69 ± 0.01	4.25	0.16 ± 0.02	1.90	0.45	1.4
			c[D-PFTFWK]			
H_2O	0.71 ± 0.05	3.72	0.16 ± 0.02	1.71	0.31	1.5
D_2O	0.66 ± 0.03	4.24	0.16 ± 0.02	1.92	0.47	1.6

[a] 25 °C, 295 nm excitation wavelength. Global analysis of data from 320 to 390 nm emission wavelength, 10-nm increments.

(44) Clore, G. M.; Gronenborn, A. M. *Protein Eng.* **1987**, *1*, 275−288.

(45) Chen, R. F.; Knutson, J. R.; Ziffer, H.; Porter, D. *Biochemistry* **1991**, *30*, 5184−5195.

effects in the three peptides indicates that intramolecular excited-state proton-transfer catalyzed by the ϵ-ammonium of lysine does not occur in c[D-PFTKWF] and c[D-PFTFWK].

The temperature dependence of the fluorescence lifetime of NATA in water has two Arrhenius factors,

$$\tau^{-1} = k_o + A_1 \exp(-E_1^*/RT) + A_2 \exp(-E_2^*/RT) \quad (7)$$

where $k_o = k_r + k_{isc}$ is the temperature-independent rate, A_i is the frequency factor, E_i^* is the activation energy, R is the gas constant, and T is temperature in K.[7] The two Arrhenius terms represent solvent quenching $k_{si} = A_1 \exp(-E_1^*/RT)$ and excited-state electron transfer from the indole ring to the amides $k_{et} = A_2 \exp(-E_2^*/RT)$. Fluorescence decays of c[D-PpYTFWF] were measured in H_2O and D_2O from 5 to 55 °C and deconvolved in single curve analyses. The long lifetime τ_1 decreased monotonically over the temperature range studied, from 5.14 ns at 7.2 °C to 1.97 ns at 55 °C in H_2O. The temperature dependence of the intermediate and short lifetimes was obscured by correlation among the decay parameters of these minor components in the three exponential fits. Plots of $\ln[\tau_1^{-1} - k_o - k_{si}]$ versus $1/T$ for the long lifetime data were made, using k_r values from Table 2 and k_{isc} and k_{si} values for NATA.[7] Arrhenius parameters obtained from the intercept and slope of the lines were: $A_2 = 1.9 \times 10^{11}$ s^{-1} and $E_2^* = 4.4$ kcal/mol in H_2O and $A_2 = 5.3 \times 10^{11}$ s^{-1} and $E_2^* = 4.9$ kcal/mol in D_2O. Electron-transfer rates calculated at 25 °C are 1.1×10^8 s^{-1} in H_2O and 1.4×10^8 s^{-1} in D_2O. The k_{et} values for the long lifetime component of c[D-PpYTFWF] are slightly lower than the values for NATA (2.0×10^8 s^{-1} in H_2O and 2.2×10^8 s^{-1} in D_2O).[7]

Excited-State Electron Transfer. Two models for producing different local environments of Trp[5] can explain the multiexponential fluorescence decay of c[D-PpYTFWF]. (1) Different lifetimes result from multiple ground-state rotamers of the tryptophan side chain as proposed by the rotamer model.[14,15] (2) Different lifetimes result from multiple conformations of the peptide backbone. The latter is unlikely because of the strong NMR evidence for a rigid backbone. Moreover, the χ_1 side chain rotamer populations of Trp[5] determined from NMR correlate very well with the relative amplitudes of the fluorescence decay. By assuming that the radiative rates of the rotamers are the same, the different lifetimes would be due to differences in the total nonradiative rate. On the basis of intermolecular quenching experiments,[8] we expect only three dynamic quenching mechanisms in c[D-PpYTFWF]: intersystem crossing, water quenching, and peptide bond quenching by excited-state electron transfer. We assume that the intersystem crossing and water quenching rates are the same for all Trp[5] rotamers and equal or similar to the rates in NATA.[7] In this scenario, the three Trp[5] lifetimes would result from differences in peptide bond quenching among rotamers. The total electron-transfer rate $k_{et}(j)$ of rotamer j is the sum of the individual electron-transfer rates from Trp[5] to each of the six peptide bonds in c[D-PpYTFWF]

$$k_{et}(j) = \sum_i k_{et}(i,j) \quad (8)$$

where $k_{et}(i,j)$ is the quenching rate of rotamer j by peptide bond i.

In a system with weak coupling between donor and acceptor, the electron-transfer rate decreases exponentially with distance r.[46] The electronic coupling of donor and acceptor in proteins may be through-space, hydrogen-bonding, or covalent.[47] Electron transfer occurs from the highest occupied molecular orbital (HOMO) of the donor to the lowest unoccupied molecular orbital (LUMO) of the acceptor. For tryptophan-containing peptides, excited indole is the electron donor. In aqueous solution, emission and therefore also electron transfer occur from the ^1L_a state.[48] The carbonyl carbon of the peptide bond is probably the electron acceptor. The covalent bond distances are the same for all rotamers. A through-bond electron transfer mechanism could not produce lifetime heterogeneity unless the through-bond electron-transfer rate were highly dependent on the orientation of the indole ring and the peptide bond. Moreover, the through-space distances between indole and various carbonyl carbons are a few Å shorter than the through-bond distances. Hence, we only consider through-space electron-transfer mechanisms. An orientation dependence of k_{et} has been shown for heme-heme intramolecular electron transfer in cytochromes, even when donor−acceptor distances were comparable in different proteins.[49] The effect of orbital overlap has been treated by several workers.[50−52] The electron-transfer rate may be expressed as a function of distance and orientation by[50,51]

$$k_{et}(i,j) = B\, f(\theta_{i,j}) \exp(-\beta r_{i,j}) \quad (9)$$

where B is a preexponential factor independent of both r and θ, $f(\theta_{i,j})$ is an orientation function, and $\beta = 1.7$ Å^{-1} is the distance decay factor commonly used for through-space electron transfer in proteins.[53] The donor HOMO of the ^1L_a state of indole is fairly well described by the LUMO of the ground state.[54,55] The acceptor LUMO is the π^* antibonding orbital of the carbonyl C═O bond. We calculate the overlap of these orbitals very crudely with the simple orientation function $f(\theta_{i,j}) = \cos^2 \theta_{i,j}$ for overlap of $S-P$ orbitals.[51] $\theta_{i,j}$ is the dihedral angle between the planes containing the indole ring and peptide bond i in rotamer j. In the spherical elephant approximation, the S orbital represents the LUMO of the indole ring, and the P orbital represents the π^* antibonding orbital of the carbonyl.

To calculate electron-transfer rates of the six possible Trp[5] rotamers in c[D-PpYTFWF] from eqs 8 and 9, we need a value for B. NATA and c[D-PpYTFWF] have the same donor−acceptor pair; therefore, we assume that the electron-transfer parameters B and β in eq 9 are about the same for both molecules. NATA mimics a tryptophan-containing peptide with peptide bonds i-1 and i on either side of the indole ring. The fluorescence decay is a single exponential with 2.9-ns lifetime at 25 °C. Presumably, the single-exponential represents a multitude of ground-state species arising from the six side chain rotamers with free rotation about each peptide bond. The k_{et} value for NATA in H_2O is almost certainly a composite value

(46) Marcus, R. A.; Sutin, N. *Biochim. Biophys. Acta* **1985**, *811*, 265−322.
(47) Beratan, D. N.; Onuchic, J. N.; Hopfield, J. J. *J. Chem. Phys.* **1987**, *86*, 4488−4498.
(48) Callis, P. R. *Methods Enzymol.* **1997**, *278*, 113−151.
(49) Makinen, M. W.; Schichman, S. A.; Hill, S. C.; Gray, H. B. *Science* **1983**, *222*, 929−931.
(50) Doktorov, A. B.; Khairutdinov, R. F.; Zamaraev, K. I. *Chem. Phys.* **1981**, *61*, 351−364.
(51) Domingue, R. R.; Fayer, M. D. *J. Chem. Phys.* **1985**, *83*, 2242−2252.
(52) Cave, R. J.; Siders, P.; Marcus, R. A. *J. Phys. Chem.* **1986**, *90*, 1436−1444.
(53) Beratan, D. N.; Betts, J. N.; Onuchic, J. N. *Science* **1991**, *252*, 1285−1288.
(54) Callis, P. R. *J. Chem. Phys.* **1991**, *95*, 4230−4240.
(55) Slater, L. S.; Callis, P. R. *J. Phys. Chem.* **1995**, *99*, 8572−8581.

Table 4. Calculated Fluorescence Lifetimes for Rotamer *j* of Trp[5] in C[D-PpYTFWF][a]

		lifetime of rotamer *j* (ns), χ_1, χ_2					
β (Å^{-1})	B (10^{12} s^{-1})	−60°, 90°	−60°, −90°	−180°, 90°	−180°, −90°	60°, 90°	60°, −90°
1.4	0.38 (0.08)	2.8 (3.9)	1.9 (2.7)	1.7 (2.7)	1.4 (2.9)	1.2 (2.8)	0.80 (2.1)
1.5	0.55 (0.13)	3.1 (4.0)	2.1 (2.6)	1.8 (2.6)	1.5 (2.8)	1.3 (2.9)	0.90 (2.1)
1.6	0.80 (0.21)	3.4 (4.0)	2.3 (2.5)	1.9 (2.6)	1.6 (2.7)	1.5 (2.9)	0.95 (2.0)
1.7	1.1 (0.33)	4.0 (4.1)	2.6(2.5)	2.0 (2.5)	1.7 (2.7)	1.7 (2.9)	1.0 (2.0)
1.8	2.0 (0.60)	3.7 (3.9)	2.4 (2.3)	1.8 (2.2)	1.6 (2.4)	1.6 (2.8)	0.92 (1.8)
1.9	3.6 (0.90)	3.6 (4.1)	2.3 (2.3)	1.6 (2.3)	1.4 (2.5)	1.5 (2.9)	0.80 (1.9)
2.0	5.8 (1.5)	3.7 (4.1)	2.3 (2.2)	1.5 (2.0)	1.3 (2.3)	1.5 (2.9)	0.78 (1.7)
2.1	9.2 (2.6)	3.8 (4.1)	2.3 (2.1)	1.5 (2.0)	1.3 (2.2)	1.5 (2.8)	0.76 (1.7)
2.2	15 (4.0)	3.9 (4.1)	2.2 (2.1)	1.4 (2.0)	1.2 (2.2)	1.5 (2.9)	0.72 (1.7)
2.3	25 (6.7)	4.0 (4.2)	2.2 (2.0)	1.3 (1.8)	1.2 (2.1)	1.5 (2.9)	0.67 (1.6)
2.4	44 (11)	3.9 (4.2)	2.0 (2.0)	1.2 (1.8)	1.1 (2.0)	1.4 (2.9)	0.60 (1.6)
2.5	75 (18)	3.9 (4.2)	2.0 (2.0)	1.1 (1.8)	1.0 (1.9)	1.4 (2.9)	0.54 (1.5)
2.6	120 (29)	4.0 (4.1)	1.9 (1.9)	1.0 (1.7)	0.93 (1.8)	1.4 (2.9)	0.52 (1.5)

[a] Numbers in parentheses calculated assuming no orientation dependence.

from these multiple species, so that B is likewise a composite value. We estimate B using the electron-transfer rate of NATA from

$$k_{et}(\mathrm{NATA}) = (B/6)\sum_j \langle f(\theta_{i-1,j})\exp(-\beta r_{i-1,j})\rangle + \langle f(\theta_{i,j})\exp(-\beta r_{i,j})\rangle \quad (10)$$

The summation over $j = 1-6$ assumes equal populations of the six canonical rotamers of the indole side chain. To simulate free rotation about the ϕ, ψ bonds in each rotamer j, 12 values of $f(\theta_{i-1,j})\exp(-\beta r_{i-1,j})$ and $f(\theta_{i,j})\exp(-\beta r_{i,j})$ for peptide bonds i-1 and i were computed and averaged. Using $k_{et}(\mathrm{NATA}) = 2.0 \times 10^8$ s^{-1} at 25 °C,[7] eq 10 gives $B = 1.1 \times 10^{12}$ s^{-1}. Assuming no orientation dependence with $f(\theta_{i,j}) = 1$, eq 10 gives $B = 3.3 \times 10^{11}$ s^{-1}.

Individual electron-transfer rates $k_{et}(i,j)$ from rotamer j of Trp[5] to peptide bond i in c[D-PpYTFWF] were calculated from eq 9, and the total electron-transfer rate $k_{et}(j)$ for each rotamer was then calculated from eq 8 (Table SI). In general, for distances >6 Å or orientations of the indole ring and the peptide bond >70°, the $k_{et}(i,j)$ values are negligible (<10^7 s^{-1}). In the six rotamers, the peptide bonds on either side of the indole ring contribute >84% of the total $k_{et}(j)$. The $k_{et}(j)$ values vary by a factor of 7 among rotamers with peptide bond quenching being fastest in the 60°, −90° rotamer and slowest in the −60°, 90° rotamer. Neglecting orientation, the $k_{et}(j)$ values vary by less than a factor of 4.

Table 4 gives the fluorescence lifetimes for the six rotamers. Lifetimes were calculated from eqs 1 and 2 with $k_{pt} = 0$, using k_r for the peptide from Table 2 and $k_{isc} + k_{si} = 8.4 \times 10^7$ s^{-1} for NATA at 25 °C.[7] For $\beta = 1.7$ Å^{-1}, the lifetimes range from 1 to 4 ns. For each χ_1 rotamer, the calculated lifetimes of the $\chi_2 = \pm 90°$ rotamers differ by less than a factor of 2. Such closely spaced lifetimes are difficult to resolve in a multiexponential decay. With this in mind, we rationalize the observed and calculated lifetimes of c[D-PpYTFWF] according to the rotamer model as follows.

(I) Assume that the rotamers do not interconvert on the fluorescence time scale, that the observed fluorescence decay amplitudes α_i equal the NMR-determined χ_1 rotamer populations, and that each χ_1 rotamer has a major χ_2 rotamer. This assigns the 4.0-ns lifetime calculated for the −60°, 90° rotamer to the observed 3.8-ns component, either the 1.7- or 2.0-ns lifetime calculated for the $\chi_1 = 180°$ rotamers to the observed 1.8-ns component, and the 1.0-ns lifetime calculated for the 60°, −90° rotamer to the observed 0.3-ns component. Case I agrees with the χ_2 rotamer populations of tryptophan zwitterion,[56] although not with the apparently uncorrelated χ_1, χ_2 rotamer populations of the cyclic peptide. To test whether Case I is consistent with the time-resolved fluorescence data, we simulated triple exponential fluorescence decays using calculated lifetimes and amplitudes equal to the respective χ_1 rotamer populations of Trp[5] in Table 1. Eight simulations using the 4.0, 1.7, and 1 ns values recovered lifetimes (amplitudes) of 3.6−3.9 (0.71 ± 0.07), 1.5−1.9 (0.16 ± 0.02), and 0.14−0.55 ns (0.13 ± 0.06) with $\langle\bar{\tau}\rangle = 3.0 \pm 0.2$ ns. Nine of 10 simulations using the 4.0, 2.0, and 1 ns values recovered lifetimes (amplitudes) of 3.4−5.7 (0.69 ± 0.06), 1.5−2.1 (0.19 ± 0.05), and 0.15−0.35 ns (0.11 ± 0.03) with $\langle\bar{\tau}\rangle = 3.0 \pm 0.5$ ns. Only one simulation recovered the 1-ns value for the short lifetime with $\bar{\tau} = 3.06$ ns.

(II) Assume that the χ_1 rotamers do not interconvert on the fluorescence time scale, that the observed fluorescence decay amplitudes equal the NMR-determined χ_1 rotamer populations, but that the observed lifetimes represent some form of average lifetime of the two χ_2 rotamers. For example, if the χ_2 rotamers interconvert rapidly, then the lifetimes would converge to a single value[14]

$$1/\tau = (k_{90} + Kk_{-90})/(1 + K) \quad (11)$$

where k_{90} and k_{-90} are the decay rates and the equilibrium constant $K = p_{-90}/p_{90}$ is the population ratio of χ_2 rotamers. A value of $K = 0.11$ was calculated from eq 11 using the observed 3.8-ns lifetime of the $\chi_1 = -60°$ rotamer and the calculated decay rates of the two χ_2 rotamers, which corresponds to 90% population for $\chi_2 = 90°$ as assumed in Case I.

Table 4 also shows the effect of β on the calculated lifetimes of the six rotamers. β values of 1.4, 1.7, and 2.6 Å^{-1} have been used for through-space electron transfer in proteins.[57−59] The −60°, 90° rotamer has the longest lifetime, and the 60°, −90° rotamer has the shortest lifetime throughout this range. As expected, the lifetime difference between these rotamers in-

(56) Dezube, B.; Dobson, C. M.; Teague, C. E. *J. Chem. Soc., Perkin Trans. 2* **1981**, 730−735.
(57) Hopfield, J. J. *Proc. Natl. Acad. Sci. U.S.A.* **1974**, *71*, 3640−3644.
(58) Jortner, J.; Bixon, M. *Electron Transfer−From Isolated Molecules to Biomolecules*, Part 1; Wiley: New York, 1999.
(59) Moser, C. C.; Keske, J. M.; Warncke, K.; Farid, R. S.; Dutton, P. L. *Nature* **1992**, *355*, 796−802.

creases with β for both orientation-dependent and orientation-independent mechanisms. Orientation has the most effect on the lifetime of the 60°, −90° rotamer and the least effect on the two $\chi_1 = -60°$ rotamers. Cases I and II predict the 3.8- and 1.8-ns lifetimes quantitatively, but not the 0.3-ns lifetime. The predictions are robust to β values between 1.7 and 2.1 Å.

Conclusions

This paper provides definitive evidence for the rotamer model of tryptophan photophysics for peptides in aqueous solution. c[D-PpYTFWF] has a rigid backbone, making side chain rotamers the only source of conformational heterogeneity. The three fluorescence decay amplitudes correlate well with the three χ_1 rotamer populations of Trp^5 determined by ^1H NMR. The three fluorescence lifetimes can be explained by differences among χ_1, χ_2 rotamers in the rate of intramolecular excited-state electron transfer from the indole ring to two to four peptide bonds in c[D-PpYTFWF]. Except for the shortest lifetime, remarkably good quantitative agreement is obtained with calculated lifetimes using a simple model and reasonable assumptions. Two relatively innocuous approximations were made to calculate fluorescence lifetimes, namely (1) The radiative, intersystem-crossing, and water-quenching rates are the same in all rotamers. (2) The intersystem-crossing and water-quenching rates are the same in NATA and c[D-PpYTFWF]. Intersystem crossing plus water quenching $k_{isc} + k_{si}$ contribute only about 30% of the average total nonradiative rate (Table 2) or 10−40% in individual rotamers (Table SI). Likewise, $k_r + k_{isc} + k_{si}$ contributes at most about 50% of the total decay rate. Small differences in these contributions would be overshadowed by the larger electron-transfer rates.

The electron-transfer calculations attempt to establish a quantitative relationship between fluorescence lifetime and molecular structure. Given the many assumptions, is the agreement between calculated and experimental lifetimes entirely fortuitous? We assumed a through-space electron transfer mechanism with orientation dependence. Electronic propagation in peptides probably involves a combination of through-space and through-bond mechanisms, like the pathway model used for protein electron transfer. Moreover, we made a number of simplifying assumptions to estimate electron-transfer rates, the most significant being: (1) Orientation dependence of electron transfer from the excited indole ring to the carbonyl carbon was approximated by overlap of $S-P$ orbitals. The assumption of a spherical molecular orbital for ^1L_a neglects the nodal structure of the ground-state LUMO.[55] (2) Distances and relative orientations were measured for canonical conformations of χ_1, χ_2 rotamers. (3) The Marcus parameter B was estimated from the electron-transfer rate of NATA and β was borrowed from ground-state electron-transfer theory. Finally, we assumed that the middle of the indole ring is the electron donor. The donor atom closest to the acceptor, indole C3 in our case, is normally used in protein electron-transfer calculations. We also did calculations with indole C3 as electron donor. Not surprisingly, there was less variation in electron-transfer rates among rotamers, factors of four with orientation and only two without orientation. Much more work with well-defined model systems is needed to place the excited-state electron-transfer calculations on firm ground.

Excited-state relaxation processes have been invoked to explain the complex fluorescence decays of proteins.[9−11] Dipolar solvent relaxation on the fluorescence time scale is amply documented for indole derivatives in viscous solvents.[9,60−62] We may exclude solvent relaxation as a source of lifetime heterogeneity in the cyclic peptides on the following two grounds: (1) The fluorescence decays of the cyclic peptides appear independent of emission wavelength. At the 10-nm resolution of our time-resolved emission spectral data, $\lambda_{max} = 350$ nm for both 3.8- and 1.8-ns components and 340 nm for the 0.3-ns component. The short lifetime component constitutes <2% of the total intensity, so its spectrum may include a contribution from the water Raman at 331 nm. (2) Solvent relaxation of tryptophan zwitterion has a 1.2-ps relaxation time in aqueous solution at room temperature.[63] It is unlikely that the relaxation time would be much slower for a fully solvent exposed tryptophan in a small peptide. On the other hand, rotamer interconversion during the lifetime of the excited state is a possibility. The good agreement between NMR-determined ground-state rotamer populations and fluorescence decay amplitudes suggests that χ_1 rotamer interconversion is slower than the fluorescence time scale, albeit faster than the NMR time scale. In molecular dynamics simulations using an all atom representation, χ_2 rotamer interconversion is faster than χ_1 rotamer interconversion.[64] The short lifetime component may be indicative of excited-state conformer interconversion.[65] If so, the lifetime heterogeneity would still be due to at least three ground-state rotamers with different lifetimes, but the amplitudes and decay times would no longer simply represent the rotamer populations and lifetimes.

Although the peptide bond is a weak intermolecular quencher of 3-methylindole fluorescence, it is an efficient intramolecular quencher in NATA[7] and the cyclic peptides. This strongly suggests that peptide bond quenching is an important quenching mechanism in proteins. The quenching rate will depend on the number, distance, and possibly orientation of peptide bonds within about 6 Å of the indole ring. Sillen et al. proposed that electron-transfer quenching by the peptide bond may be the main determinant of the lifetime of tryptophan in proteins in the absence of strong quenchers.[13] They used molecular dynamics to determine tryptophan rotamer populations and Marcus theory to predict the three fluorescence lifetimes of two single tryptophan proteins. The details of their lifetime calculations differ from those presented here. In c[D-PpYTFWF], the peptide bond is assumed to be the only intramolecular quenching group. Although phenylalanine is not an intermolecular quencher of 3-methylindole fluorescence,[8] the phenyl ring has been proposed to be a highly efficient intramolecular quencher of buried tryptophans in proteins.[12] The presumed quenching mechanism involves an atypical NH···π hydrogen bond, which requires a particular orientation of the indole nitrogen relative to the phenyl ring. There are three other aromatic residues in c[D-PpYTFWF] besides tryptophan: $pTyr^2$, Phe^4, and Phe^6. However, these

(60) Milton, J. G.; Purkey, R. M.; Galley, W. C. *J. Chem. Phys.* **1978**, *68*, 5396−5403.
(61) Lakowicz, J. R.; Cherek, H.; Bevan, D. R. *J. Biol. Chem.* **1980**, *255*, 4403−4406.
(62) Meech, S. R.; Phillips, D.; Lee, A. G. *Chem. Phys. Lett.* **1982**, *92*, 523−527.
(63) Shen, X.; Knutson, J. R. *J. Phys. Chem. B* **2001**, *105*, 6260−6265.
(64) Gordon, H. L.; Jarrell, H. C.; Szabo, A. G.; Willis, K. J.; Somorjai, R. L. *J. Phys. Chem.* **1992**, *96*, 1915−1921.
(65) McMahon, L. P.; Yu, H.-T.; Vela, M. A.; Morales, G. A.; Shui, L.; Fronczek, F. R.; McLaughlin, M. L.; Barkley, M. D. *J. Phys. Chem. B* **1997**, *101*, 3269−3280.
(66) Kirby, E. P.; Steiner, R. F. *J. Phys. Chem.* **1970**, *74*, 4480−4490.

residues are probably not intramolecular quenching groups in the cyclic peptides. First, substitution of either phenylalanine by lysine in c[D-PFTKWF] and c[D-PFTFWK] has no effect on fluorescence quantum yield and lifetimes. Second, molecular modeling shows that the particular conformation for NH$\cdots\pi$ hydrogen bonding is equally possible in all tryptophan χ_1 rotamers. Last, NH$\cdots\pi$ hydrogen bonding is not likely to occur in aqueous solution.

Acknowledgment. This work was supported by NIH Grant GM42101.

Supporting Information Available: Table of electron transfer rates for rotamer *j* of Trp^5 of c[D-PpYTFWF] (PDF). This material is available free of charge via the Internet at http://pubs.acs.org.

JA0167710